Deep Learning based Fault Classification Algorithm for Roller Bearings using Time-Frequency Localized Features

Arka Bera
Dept. of Mechanical Engineering
National Institute of Technology, Durgapur
Durgapur, India
ab.17u10648@btech.nitdgp.ac.in

Arindam Dutta
Dept. of Computational and Data Science
Indian Institute of Science, Bangalore
Bangalore, India
arindamdutta@iisc.ac.in

Ashis K. Dhara
Dept. of Electrical Engineering
National Institute of Technology, Durgapur
Durgapur, India
ashis.dhara@ee.nitdgp.ac.in

2021 International Conference on Computing, Communication, and Intelligent Systems (ICCCIS) | 978-1-7281-8529-3/20/$31.00 ©2021 IEEE | DOI: 10.1109/ICCCIS51004.2021.9397072

***Abstract*—The paper proposes an algorithm to classify different conditions of a bearing based on vibration data using a deep convolutional neural network. Spectrograms of vibration data are generated by means of Short-time Fourier Transform and then provided as input to a convolutional neural network. The network is successful in predicting the health condition of the bearing from the spectrograms and achieves a classification accuracy of 97%. The trained model is then tested on a different dataset and the model is able to predict the classes with an accuracy of 96%. The proposed model is finally compared with pre-existing models to evaluate its performance and the results demonstrate the state of the art performance of our proposed algorithm.**

***Index Terms*—Condition monitoring, Spectrogram, Convolutional Neural Networks**

I. Introduction

Roller bearings are an integral part of any machinery having rotating mechanisms. Bearings enable smooth operation of shafts and axles, and provide efficient means to reduce friction between moving parts. Longevity of bearings is considered an essential parameter in the design of bearings. Factors such as temperature [1], lubrication [2], installation and maintenance play a significant role in determining the life of a bearing.

Significant studies have been conducted to estimate the operating life, known as L10 life, of a bearing [3]. However, such work is generally statistical and thus, the duration of smooth operation of a bearing is often probabilistic. Failure in one or more components of a bearing can cause a considerable amount of damage to machine parts. Thus, it is of paramount interest to monitor the health of a bearing, also known as condition monitoring [4]. This can be achieved by several means.

The simplest means of checking the health condition of a bearing is visual inspection. For visual inspection, it is necessary to put apart a machine to investigate the particular machine part in question. This is a tedious task, and often time consuming. Oil analysis [5] is a method in which lubricants from machine parts are tested for changes. Wear and tear, overheating, etc can lead to changes in composition of the oil, as well as deposition of contaminants. Another method is vibration analysis [6], [7], where accelerometers or other sensors are used to collect vibration data from bearing housing, which is then analyzed for changes in health condition. Wear and tear of bearings, misalignments, improper design or installment, etc produce vibrations which are significantly different from those produced by healthy bearings. Infrared thermography [8], [9] is a method in which images of thermal radiation from machine parts are used for analysis of health conditions of machinery. As failure occurs in machine parts, anomalies in thermographic images and temperature differences become more prominent. Acoustic analysis [10], [11], also known as ultrasonic monitoring, makes use of sound waves having high frequency to detect subtle changes in friction that other methods such as vibration analysis or infrared thermography cannot detect. Apart from these, there are several methods for condition monitoring of bearings and other machine parts, such as radiography, ferrography [12], laser interferometry, electric monitoring and electromagnetic measurement.

Of these methods, vibration analysis of bearings is a widely used approach for condition monitoring of bearing health conditions [13]. Vibration signals are easy to record and contain concise information regarding the health condition of the bearings. However, in normal operating conditions, the vibration data is often contaminated by surrounding noise. Although, in recent times, deep learning models have been implemented for solving the task at hand by using vibration data [14], [15], these algorithms are memory heavy and fail to serve the purpose of pragmatic implementation.

Our major contributions in this paper are:

- We propose a light-weight CNN for condition monitoring of bearings using vibration data. The vibration data is first converted from the time-domain into 2D images, called spectrograms. The CNN is trained and subsequently validated to identify between the different classes of health conditions.
- We also compare our results against pre-existing state of the art models such as VGG [16], Residual Network [17]

ISBN: 978-1-7281-8529-3/21/$31.00 ©2021 IEEE

and Inception Network [18].

The remaining paper is organized as: Section II gives a complete overview of the Preprocessing that was done for the algorithm. Section III provides details on the Experiments and Results obtained while Section IV concludes the paper.

II. Preprocessing

A. Test rig

The dataset was generated using the experimental setup as shown in Fig. 1. The experiments are conducted in a SpectraQuest simulator for machinery fault (MFS-PK5M). A motor drives the shaft and the rotational speed is regulated by an AC drive. ER16K ball bearings are used to support the shafts. There are 2 such bearings: i) the left one is a healthy bearing, ii) the right one is the experimental bearing having varying health conditions. An ICP Accelerometer (Model 623C01) is attached to the housing of the experimental bearing to record the vibrational data. The shaft rotational speed is measured using an incremental encoder (EPC model 775).

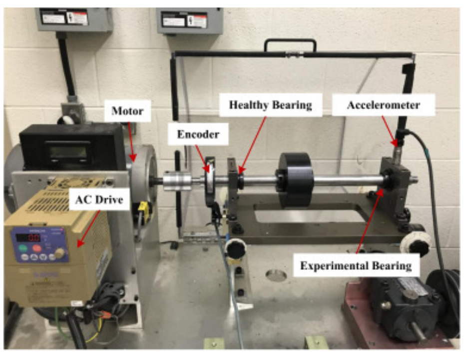

Fig. 1: Test rig for recording vibration data [19]

Every type of fault has a specific Fault Characteristic Frequency (FCF) [20]. FCF is a parameter for detection and diagnosis of bearing faults. FCF is proportional to the operating rotational frequency. The bearing structural parameters, given in Table I, play a significant role in the determination of FCF.

TABLE I: Structural Parameters of Experimental Bearing

Bearing type	Pitch diameter	Ball diameter	Number of balls	BPFI	BPFO
ER16K	38.52 mm	7.94 mm	9	5.43f$_r$	3.57f$_r$

BPFO is Ball-Pass Frequency for Outer Range, BPFI is Ball-Pass Frequency for Outer Range, and f$_r$ is the shaft rotational frequency.

The data is acquired by the NI data acquisition board (NI USB-6212 BNC). Each recorded dataset contains two channels, both saved in one '.mat' file. The accelerometer records vibration data, stored in 'Channel_1', while the encoder records rotational speed data, stored in 'Channel_2'. Signals are recorded at 2,00,000 Hz and the duration is 10 seconds.

B. Data Set

The dataset contains vibrational signals collected from a bearing having varying health conditions. The rotational speed of the bearing varies with time. The complete dataset is available at [19].

The conditions of the bearing are as follows: i) healthy bearings, ii) bearings with defect in inner race, iii) bearings with defect in outer race, iv) bearings having ball defect, v) bearings having a combination of defects in inner race, outer race and ball.

The rotational speed of the bearing varies as: i) increasing, ii) decreasing, iii) increasing and then decreasing , iv) decreasing and then increasing.

Thus there are 20 different operating conditions. For each operation setting, 3 sets of readings have been taken with minor variations in parameters to ensure that the data is unequivocal. Thus, there are a total of 60 datasets. Each dataset has two channels: i) 'Channel_1' is vibration data, recorded by means of accelerometer, ii) 'Channel_ 2' is rotational speed of bearing, recorded by the encoder. The data is sampled at 2,00,000 Hz for a duration of 10 seconds. Cycles per Revolution (CPR) of the encoder is 1024.

The proposed CNN is trained and tested using the datasets having increasing rotational speed. The trained model is thereafter evaluated using datasets having decreasing speed. "Channel_1" of the datasets is used to generate spectrograms. The entire length of the vibration signal is divided into subparts of 1000 Hz. MATLAB is used to convert this vibrational data into spectrogram images.

C. Short-time Fourier Transform

Short-time Fourier Transform (STFT) is a variant of Fourier transform and is used to calculate the sinusoidal frequency as well as the phase content of adjacent segments of a signal as it varies over a period of time. STFTs are computed by dividing a longer time response signal into shorter segments having equal intervals, and then operating Fourier transform on each of the shorter segments. Thus, the Fourier spectrum is obtained over a range of shorter segments, which can then be used to plot a spectrogram or a waterfall plot. There are two types of STFT: i) Continuous-time STFT and ii) Discrete-time STFT.

For Continuous-time STFT, a window function is selected which is non-zero for a short period of time, such as Hann or Gaussian window. The function to be transformed is multiplied by the window function. As the window is slid along the time axis, Fourier transform of the resultant signal is taken. Thus, a two-dimensional representation of the signal is obtained. The mathematical expression for this operation is given as:

$$STFT(x(t))(\tau, \omega) = \int_{-\infty}^{\infty} w(t-\tau)x(t)e^{-j\omega t}dx \quad (1)$$

where $w(\tau)$ is the window function and $x(t)$ is the signal which is to be transformed. $X(\tau, \omega)$ is the Fourier transform of $x(t)w(t-\tau)$, a complex function which represents the

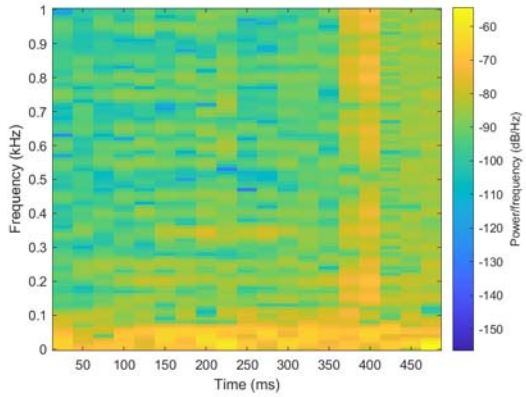

(a)

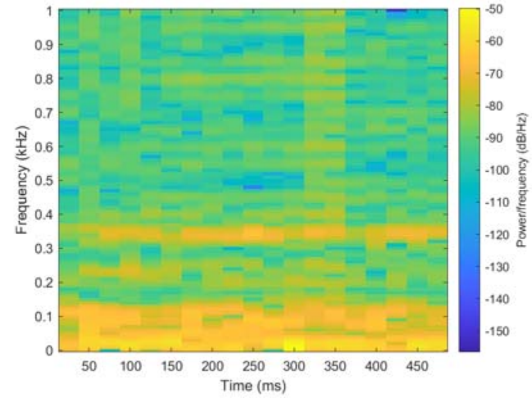

(b)

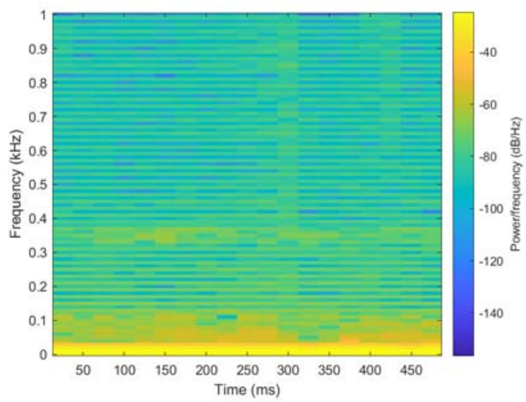

(c)

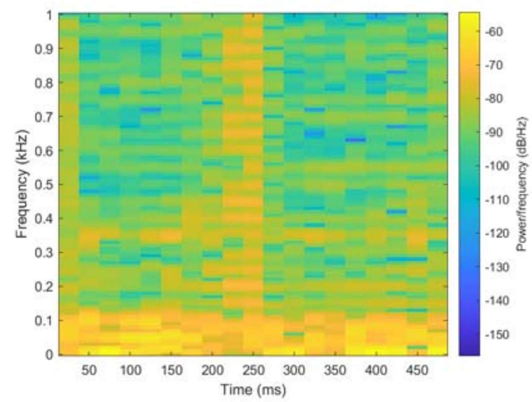

(d)

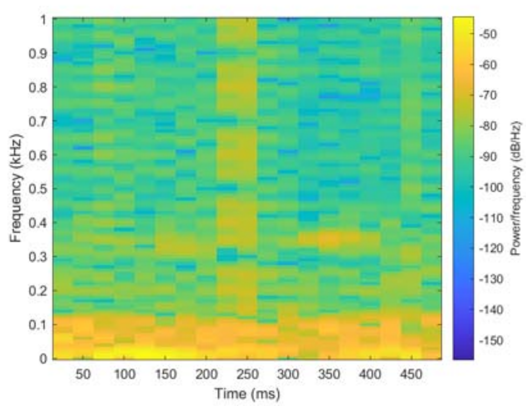

(e)

Fig. 2: Spectrograms generated for different health conditions of bearings (a) Healthy bearing (b) Bearing with defect in a ball (c) Bearing with defect in inner race (d) Bearing with defect in outerrace (e) Bearing with combination of all defects

magnitude and phase of the signal over a given range of time and frequency.

Squaring the value of the STFT gives the spectrogram representation of the Power Spectral Density of the original function. The mathematical expression is:

$$STFT\{x(t)\}(\tau,\omega) \equiv |X(\tau,\omega)|^2 \tag{2}$$

D. Spectrogram Generation

A spectrogram is a graphical representation of the signal strength. It represents the spectrum of frequencies that constitute a time-varying signal. When represented as a three-dimensional plot, a spectrogram can be termed as 'waterfall'. A spectrogram is an RGB image, usually depicted as a heat map. The intensity of various frequencies is shown by means

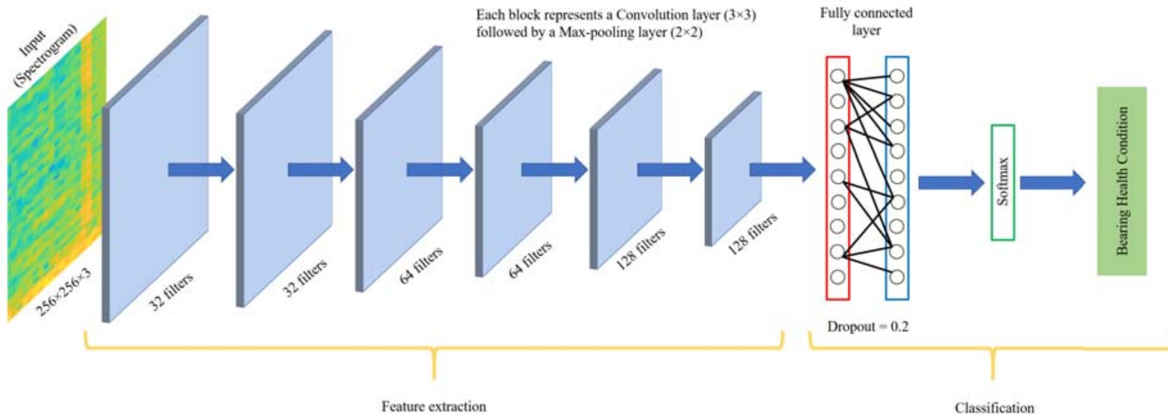

Fig. 3: Schematic of CNN architecture for classification of roller bearing health conditions using spectrograms

of varying colours and brightness.

Spectrograms have been used widely in fields such as music [21], language detection [22], sonar and radar, speech processing [23], etc. The proposed model uses spectrograms generated from time-response signals to classify between bearings of varying health conditions.

Spectrograms can be obtained by means of: i) an optical spectrometer, an instrument which measures the properties of light over a specific portion of electromagnetic spectrum, ii) band-pass filters (BPF), a device that allows passage of frequency in a given range and attenuates frequencies outside that range, iii) by Fourier transform, where a signal in time domain is converted into the frequency domain.

The spectrograms for the work have been generated by means of Short-time Fourier Transform (STFT) using MATLAB R2020a [24]. A dataset in time domain has been subdivided into sections of 1000 Hz. Thus, each dataset gives 2000 sections. Henceforth, STFT has been applied to each of these sections with a Hamming window of size 100 to obtain spectrograms of the signal.

There are 3 sets of readings for each health condition of a bearing (with increasing rotational speed). Thus the total number of spectrograms generated for each class of bearings is 6,000. The total dataset consisting of all health conditions of a bearing (with increasing rotational speed) is 30,000. 4,200 images from each health condition (21,000 in total) are chosen randomly and used for training the network. 1,800 images from each health condition (9,000 in total) are used for validation. Spectrograms generated for each health condition of bearing is shown in Fig.2.

Thereafter, spectrograms are generated for one dataset of each of the health conditions of a bearing with decreasing rotational speed. Out of 10,000 images generated, 5,000 are selected randomly and used to evaluate the performance of the trained model.

III. Experiments and Results

A. Training of CNN Model

The dataset consisting of spectrograms of bearings having different health conditions was prepared using MATLAB. The spectrograms were then provided as input to a CNN that was developed from scratch.

The proposed model has 6 convolutional layers, with a max-pooling layer after each CL. Thus there are a total of 12 layers. Max-pooling is chosen as it has been found to work well in image classification problems. ReLU is used as an activation function for each CL. The kernel size is set as 3×3, which makes the CNN simple yet robust and reduces computational time of the network. The schematic of the CNN model is given in Fig.3.

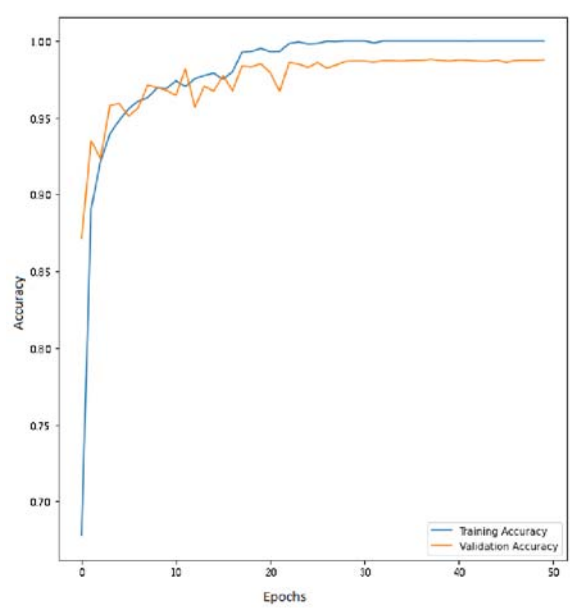

Fig. 4: Variation of accuracy with epoch

There are 2 fully connected layers. The first layer has an input size of 256 nodes and ReLU activation function. A dropout layer having dropout rate of 0.20 is implemented to prevent over-fitting of the model. The output layer has 5 classes as output. Softmax activation layer is used to obtain the probability of each class. The Softmax function takes the input vector of real numbers and converts it into a vector of real numbers having a sum of 1. Thus the probability of each class can be obtained. The Softmax activation function is given as:

$$\sigma(z)_i = \frac{e^{z_i}}{\sum_{j=1}^{K} e^{z_j}}, \quad \text{for i = 1, 2, 3 ... } K \tag{3}$$

Stochastic gradient descent is used to optimize the parameters of the model. The loss function used is categorical cross-entropy.

$$Loss(y, \hat{y}) = -\frac{1}{5}\sum_{i}^{5} y_i \log \hat{y}_i \tag{4}$$

The model was allowed to train for 50 epochs as from various tests, convergence was seen after 30 epochs. The model provided a prediction accuracy of 97%, which shows that the model is consistently able to differentiate between the different classes. The variation of training accuracy and validation accuracy is plotted against epochs in Fig. 4.

B. Evaluating Performance of CNN Model

The trained network was used to predict the classes of the test set consisting of spectrograms of bearings subjected to decreasing speed. 1,000 images of each health condition of a bearing (5,000 in total) were used to evaluate the performance of the model. Classification accuracy of 95.88% was obtained, thus proving that the pre-trained model is able to work with new datasets.

The original training dataset was then used to train pre-existing models, namely VGG16, Residual Network (ResNet50V2) and Inception Network (InceptionV3). The trained models were tested using the test set of spectrograms of bearings subjected to decreasing speed. The results have been compared in Table II.

TABLE II: Comparison of performance of CNN models

Model	Classification accuracy	Trainable parameters	Compression ratio
Proposed CNN	95.88%	419,621	1
VGG16	97.34%	165,738,309	395
ResNet50V2	96.18%	23,575,045	56
InceptionV3	95.52%	21,778,597	52

It is seen that training in VGG16, ResNet50V2 and InceptionV3 takes much longer than in the model proposed in this paper. The former networks are more complex and require higher computational capabilities as is evident from the compression ratios. The proposed model is simple yet robust and has a performance comparable to the pre-existing models, in much shorter time and has lesser computational demands.

IV. Conclusion

With the onset of Industry 4.0 standards, condition monitoring has become an essential component for maintenance of industrial machinery and equipment. By virtue of this paper, we propose a novel fault classification scheme in roller bearings. Although this paper explores a method of classification of pre-recorded vibrational data of roller bearings, owing to it being memory efficient as compared to state of the art architectures, it can be applied for online maintenance of the equipment by proper use of electronics and instrumentation. Thus, a method of preventing catastrophic failure of machinery during working is developed. The proposed model, though simple, is very effective in classifying the varying health conditions of the bearing. The trained model can be used to identify the health conditions of bearings having different ranges of rotational frequency.

V. Future work

The current work does not take into consideration the changes that would be effected due to noise from other equipment. For that, more investigative research work needs to be carried out and this paper can be an effective starting point. Further, in our future works, we will try to implement one-shot classification [25] schemes for the same problem in order to check if the proposed problem can be solved with minimal data.

References

[1] D. Zheng, W. Chen, and D. Zheng, "An enhanced estimation on heat generation of angular contact ball bearings with vibration effect," *International Journal of Thermal Sciences*, vol. 159, p. 106610, 2020.

[2] Y. Liu, W. Wang, T. Qing, Y. Zhang, H. Liang, and S. Zhang, "The effect of lubricant temperature on dynamic behavior in angular contact ball bearings," *Mechanism and Machine Theory*, vol. 149, p. 103832, 2020.

[3] D. Koulocheris, A. Stathis, T. Costopoulos, and D. Tsantiotis, "Experimental study of the impact of grease particle contaminants on wear and fatigue life of ball bearings," *Engineering Failure Analysis*, vol. 39, pp. 164–180, 2014.

[4] N. Tandon, G. Yadava, and K. Ramakrishna, "A comparison of some condition monitoring techniques for the detection of defect in induction motor ball bearings," *Mechanical Systems and Signal Processing*, vol. 21, no. 1, pp. 244–256, 2007.

[5] W. Wang and W. Zhang, "A model to predict the residual life of aircraft engines based upon oil analysis data," *Naval Research Logistics (NRL)*, vol. 52, no. 3, pp. 276–284, 2005.

[6] M. Patil, J. Mathew, P. Rajendrakumar, and S. Desai, "A theoretical model to predict the effect of localized defect on vibrations associated with ball bearing," *International Journal of Mechanical Sciences*, vol. 52, no. 9, pp. 1193–1201, 2010.

[7] L. D. Meyer, F. F. Ahlgren, and B. Weichbrodt, "An Analytic Model for Ball Bearing Vibrations to Predict Vibration Response to Distributed Defects," *Journal of Mechanical Design*, vol. 102, pp. 205–210, April 1980.

[8] C. Meola and G. M. Carlomagno, "Recent advances in the use of infrared thermography," *Measurement Science and Technology*, vol. 15, pp. R27–R58, July 2004.

[9] D.-Y. Kim, H.-B. Yun, S.-M. Yang, w.-T. Kim, and D.-P. Hong, "Fault diagnosis of ball bearings within rotational machines using the infrared thermography method," *Journal of the Korean Society for Nondestructive Testing*, vol. 30, pp. 558–563, January 2010.

[10] M. Entezami, E. Stewart, J. Tutcher, W. Driscoll, R. Ellis, G. Yeo, Z. Zhang, C. Roberts, T. Kono, and S. Bayram, "Acoustic analysis techniques for condition monitoring of roller bearings," in *6th IET Conference on Railway Condition Monitoring (RCM 2014)*, pp. 1–8, 2014.

[11] L. Rogers, "The application of vibration signature analysis and acoustic emission source location to on-line condition monitoring of anti-friction bearings," *Tribology International*, vol. 12, no. 2, pp. 51–58, 1979.

[12] T. Wu, J. Mao, G. Dong, H. Xu, and Y. Xie, "Journal bearing wear monitoring via on-line visual ferrography," *Advanced Materials Research*, vol. 44-46, pp. 189–194, June 2008.

[13] D.-T. Hoang and H.-J. Kang, "Rolling element bearing fault diagnosis using convolutional neural network and vibration image," *Cognitive Systems Research*, vol. 53, pp. 42–50, 2019.

[14] R. Yang, M. Huang, Q. Lu, and M. Zhong, "Rotating machinery fault diagnosis using long-short-term memory recurrent neural network," *IFAC-PapersOnLine*, vol. 51, no. 24, pp. 228–232, 2018.

[15] Y. Yang, H. Zheng, Y. Li, M. Xu, and Y. Chen, "A fault diagnosis scheme for rotating machinery using hierarchical symbolic analysis and convolutional neural network," *ISA Transactions*, vol. 91, pp. 235–252, 2019.

[16] K. Simonyan and A. Zisserman, "Very deep convolutional networks for large-scale image recognition," *arXiv:1409.1556*, 2015.

[17] K. He, X. Zhang, S. Ren, and J. Sun, "Identity mappings in deep residual networks," *arXiv:1603.05027*, 2016.

[18] C. Szegedy, V. Vanhoucke, S. Ioffe, J. Shlens, and Z. Wojna, "Rethinking the inception architecture for computer vision," in *2016 IEEE Conference on Computer Vision and Pattern Recognition (CVPR)*, pp. 2818–2826, 2016.

[19] H. Huang and N. Baddour, "Bearing vibration data collected under time-varying rotational speed conditions," *Data in Brief*, vol. 21, pp. 1745–1749, 2018.

[20] R. B. Randall and J. Antoni, "Rolling element bearing diagnostics—a tutorial," *Mechanical Systems and Signal Processing*, vol. 25, no. 2, pp. 485–520, 2011.

[21] A. Dutta, D. Sil, A. Chandra, and S. Palit, "Cnn based musical instrument identification using time-frequency localized features," *Internet Technology Letters*, p. e191, 2020.

[22] H. Mukherjee, S. Ghosh, S. Sen, O. S. Md, K. C. Santosh, S. Phadikar, and K. Roy, "Deep learning for spoken language identification: Can we visualize speech signal patterns?," *Neural Computing and Applications*, pp. 8483–8501, 2019.

[23] A. Satt, S. Rozenberg, and R. Hoory, "Efficient emotion recognition from speech using deep learning on spectrograms," in *Interspeech*, pp. 1089–1093, August 2017.

[24] https://in.mathworks.com/help/signal/ref/spectrogram.html Accessed: 10th August, 2020.

[25] G. Koch, R. Zemel, and R. Salakhutdinov, "Siamese neural networks for one-shot image recognition," in *ICML deep learning workshop*, vol. 2, 2015.